Asian J. Exp. Sci., Vol. 22, No. 2, 2008; 167-176

Oxidation of Zr-based Bulk Amorphous and Nanocrystalline Alloys

S. K. Sharma
Department of Physics
Malaviya National Institute of Technology,
Jaipur - 302 017, India
E-mail : *sksh@datainfosys.net*

Abstract : Novel multicomponent Zr-based alloys like Zr-Ti-Cu-Ni-Be and Zr-Cu-Ni-Al form an important class of bulk metallic glasses with some interesting applications. Nanocrystalline forms of these alloys have been obtained by thermal annealing. Interest in bulk amorphous alloys and their nanocrystalline forms has considerably grown in recent times due to their ability to offer scope for carrying out research investigations in amorphous, supercooled liquid and nanocrystalline states of a bulk glassy alloy. Despite several studies done on the oxidation behaviour of conventional melt-spun amorphous alloys, very few studies are available on oxidation of bulk metallic glasses. The paper describes the current status of oxidation research in bulk amorphous alloys and their nanocrystalline forms obtained after annealing. Some novel results from the author's recent work carried out on oxidation of the bulk amorphous alloy $Zr_{65}Cu_{17.5}Ni_{10}Al_{7.5}$ in air in its amorphous and the supercooled liquid states in the temperature range 573 K- 663 K using X-ray photoelectron spectroscopy (XPS) will also be presented.

Key words : X-ray photoelectron spectroscopy, Oxidation, Zr-based Bulk Amorphous, Nanocrystalline, Alloys

Introduction

Bulk amorphous alloys show a fairly wide temperature range between glass transition and the crystallization temperature and a remarkable resistance to crystallization. The bulk metallic glasses require cooling rates of about 1-100 K/s or less unlike conventional melt-spun metallic glasses which require very high cooling rates of about 10^6 K/s for processing (Zhang *et al.*, 1991). The interest in bulk amorphous glasses has considerably grown in recent times due to their ability to offer the scope for carrying out research investigations both in the amorphous and the supercooled liquid states of a glassy alloy. Novel multicomponent Zr-based alloys like Zr-Ti-Cu-Ni-Be and Zr-Cu-Ni-Al form an important class of bulk metallic glasses with some interesting applications (Jhonson, 1996).

In contrast to several studies done on the oxidation behaviour of conventional melt-spun amorphous alloys (Hashimoto, 1983; Asami *et al.*, 1995; and references therein), not many studies are available on oxidation of bulk metallic glasses (Kiene *et al.*, 1999; Sharma *et al.*, 2001; Dhawan *et al.*, 2001; Sun *et al.*, 1996; Triwikantoro *et al.*, 1999; Koester *et al.*, 2001; Dhawan *et al.*, 2003; Tam and Shek, 2005). In one of the early investigations on high temperature oxidation of the bulk amorphous alloy $Zr_{60}Al_{15}Ni_{25}$ in air it was suggested that the growth of the oxide is controlled by Ni back-diffusion in the alloy (Sun *et al.*, 1999). Contrary to these observations Triwikantoro *et al.*, (1999) investigated the oxidation of several Zr-based amorphous alloys (Zr-Cu-Ni-Al) in air and reported the presence of Cu and Ni in the oxide scale. In another investigation

from the author's laboratory on oxidation of the bulk amorphous alloy $Zr_{65}Cu_{17.5}Ni_{10}Al_{7.5}$ (Dhawan *et al.*, 2003), a mechanism for its oxidation in air was proposed suggesting that the back diffusion of Ni, and possibly Cu also, is the rate limiting process during the oxidation of the alloy in the amorphous or the glassy state, while oxidation process in the supercooled liquid state is more likely dominated by the diffusion of oxygen through the oxide layer. This mechanism was verified (Dhawan *et al.*, 2007) by obtaining information about the presence of various alloy constituents, especially Ni and Cu, in the oxide film using Ar+ ion sputtering for depth profiling in conjunction with the technique of X-ray photoelectron spectroscopy (XPS). Zr-based bulk amorphous alloys are known to possess nanocrystalline phases (Koester and Triwikantoro, 1999) and some investigations on oxidation of these phases have also been reported in the literature (Koester *et al.*, 1999; Koester *et al.*, 2001; Spassov and Tzolova, 1996). A discussion on results obtained on oxidation of Zr-based bulk amorphous alloys in the author's laboratory and those reported in the literature is presented in the paper.

Experimental

The oxidation kinetics was investigated using the technique of thermogravimetric mass analyzer (TGA). For this a small piece of the alloy specimen, weighing typically few mg, was cut from amorphous ribbon (10 mm wide x 30 μm thick) of the alloy and was put on the pan of a thermo-balance of thermogravimetric analyser (Model TGA 7, Perkin Elmer). The mass gain (in g) with time (in min) during oxidation in air environment at a given temperature (T) in the temperature range 591-732 K was continuously monitored using a computer interfaced with the system. The details of the experimental conditions are presented elsewhere (Dhawan *et al.*, 2001).

In order to check whether the oxidation kinetics followed the parabolic growth law ($\Delta w = Kt1/2$, where Δw represents mass gain, t oxidation time and K parabolic rate constant), plots of the mass gain per unit area (g/cm^2) versus square root of time ($s^{1/2}$) at different temperatures (591-732 K) were obtained from these experiments. The amorphous and the supercooled liquid states of the bulk alloy were identified using the reported T-T-T diagram for this alloy (Knorr, 1999). During this analysis it was ensured that the ranges for time and temperature for identifying the amorphous and the supercooled liquid states lie well within those mentioned on the diagram. In the plots of mass gain per unit area versus square root of time different slopes were observed for the amorphous and the supercooled liquid states which yielded the values of the parabolic rate constant K in the respective states. The logarithm of the slope K ($\ln K$) [measured from the linear portion of the mass gain per unit area versus square root of time plots] was plotted against the reciprocal of the oxidation temperature ($1/T$) , thus yielding the Arrhenius plots ($K = K_0 e^{-Q/kT}$; k is the Boltzmann constant) from which the values of the activation energy (Q) and pre-exponential factor (K_0) were obtained for both the amorphous and the supercooled liquid states. Additionally, the isochronal TGA run of the specimen was also taken indicating glass transition for the alloy at 650 K at a heating rate of 10 K/min.

For XPS measurements another set of specimens was prepared in the following manner. Specimens of size (10 mm x 15 mm) were cut from the as-cast amorphous ribbon (10 mm wide x 30 μm thick) of the bulk amorphous alloys $Zr_{65}Cu_{17.5}Ni_{10}Al_{7.5}$. The samples were first cleaned ultrasonically in acetone and ethanol and later dried under a jet of pressurised air. These samples were put in an open-ended quartz tube which was inserted in a tubular furnace and annealings were performed at 573 K for 20 hours, 603 K for 8 hours, 633 K for 3 hours and 663 K for 1 hour in dry air environment inside the open-ended quartz tube. As the oxidation was carried out ex-situ in a furnace it was not possible to remove the native oxide layer from the specimens by carrying out ion beam sputter cleaning or scribing in a vacuum chamber. The study of the native oxide formed on this alloy has earlier been reported in another investigation (Sharma *et al.*, 2001). Again the choice of time-temperature combination for annealing was made on the basis of the results obtained in our previous investigation (Dhawan *et al.*, 2001) and the known T-T-T diagram for this alloy (Knorr, 1999) so that the alloy $Zr_{65}Cu_{17.5}Ni_{10}Al_{7.5}$ remained after oxidation treatment either in the amorphous (573 K and 603 K) or in the supercooled liquid state (633 K and 663 K) and did not crystallize during annealing. Then the annealed samples were taken out of the furnace and the shiny side (free surface during melt- spinning of the alloy) was analysed by X-ray photoelectron spectroscopy (XPS). The XPS measurements were done using an electron spectrometer (VG MK II) equipped with a non-monochromatic Mg K_{α} source energy (h? = 1253.6 eV) in a base pressure better than 1.0×10^{-10} m-bar in the analysis chamber and a hemispherical electron analyser at a pass energy of 50 eV. XPS peaks for constituent elements: Zr 3d, Al 2s, Cu 2p and Ni 2p were recorded along with the XPS peaks for O 1s and C 1s. The sub-surface layers in oxide films were analysed by performing sequential sputtering using argon ions (Ar^+) of 5.0 keV energy. A typical mean sputtering rate of 0.71 nm/min was obtained at this energy of argon ions (Ar^+) on the basis of sputter-rate versus depth scale calibration measurements.

Results and Discussion

Fig. 1 shows some typical TGA plots of mass gain per unit area (g/cm^2) versus square root of oxidation time ($s^{1/2}$) for the amorphous alloy $Zr_{65}Cu_{17.5}Ni_{10}Al_{7.5}$ at several temperatures. A single linear region (e.g. in the plot at 591 K) corresponds to the amorphous or the glassy state of the alloy as suggested by the known T-T-T diagram for this alloy. On the other hand two different linear regions (e.g. as observed in the plots at 628 K, 646 K and 664 K), correspond to the amorphous and supercooled liquid states according to the T-T-T diagram for the alloy. The linear regions corresponding to the amorphous state at different temperatures are also shown separately in an expanded plot in Fig. 2. It is noted from Fig. 2 that with increase in temperature the linear region corresponding to the amorphous state is progressively reduced and at temperatures higher than 664 K only a single linear region corresponding to the supercooled liquid state is observable. The linear region corresponding to the amorphous state at 664 K is too short to be seen in Fig. 1 and is visible in an expanded plot shown in Fig. 2. The plots at 681 K and 684 K (not shown

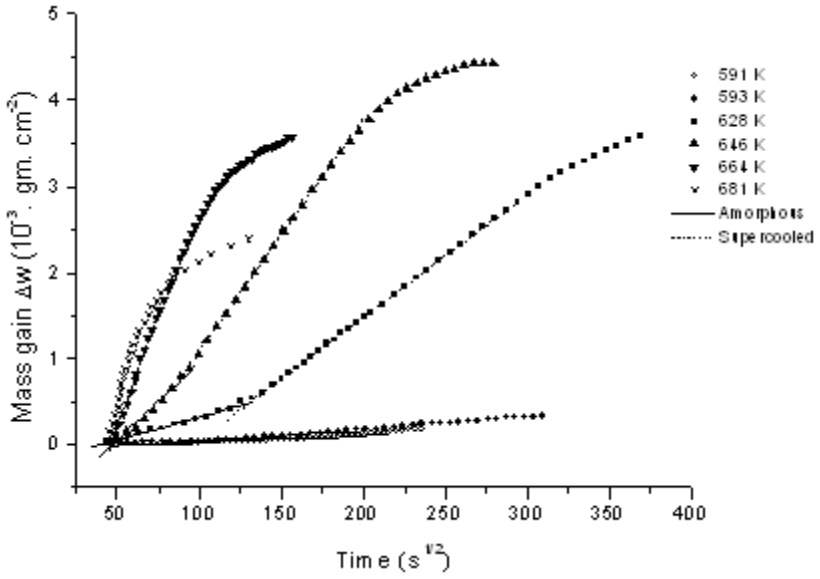

Fig. 1 : Plots of mass gain (g/cm^2) versus square root of time (s$^{1/2}$) at various temperatures. The solid line corresponds to the linear fit to the data in the amorphous state while the dashed line represents the linear fit to the data in the supercooled liquid state.

Fig. 2 : Plots of mass gain (g/cm^2) versus square root of time in (s$^{1/2}$) at different temperatures showing linear region corresponding to the amorphous state in an expanded plot.

in the figure) also show a single linear region corresponding to the supercooled liquid state and at these temperatures the region corresponding to the amorphous state is not observed. At further higher temperatures (723 K and 732 K) glass gets crystallized thus indicating no amorphous or supercooled liquid state. It is thus observed from Fig. 2 and Fig. 3 that, the mass gain per unit area agrees reasonably well with linear variation of square root of oxidation time for both the amorphous and the supercooled liquid states of the alloy $Zr_{65}Cu_{17.5}Ni_{10}Al_{7.5}$. This suggests that for temperatures and annealing times employed in this investigation the oxidation reaction kinetics obeys a parabolic rate law ($\Delta w = K t^{1/2}$) in the amorphous as well as in the supercooled liquid states.

The slopes of the linear regions in parabolic plots, as shown in Fig. 1 and Fig. 2, yield the values of the parabolic rate constant K at a given temperature. Fig 3 represents the Arrhenius plot ($K=K_o\, e^{-Q/kT}$) between the logarithm of slope K and $1/T$, thus yielding the values of the activation energy (Q) for oxidation in both the amorphous and the supercooled liquid states. The value of the activation energy needed in the case of supercooled liquid state (1.20 ± 0.1)eV is significantly lower than that in the amorphous state (1.80 ± 0.1) eV.

The value of the activation energy obtained in the case of amorphous phase (1.80 eV) is close to the value of the activation energy (1.90 eV) for the diffusion

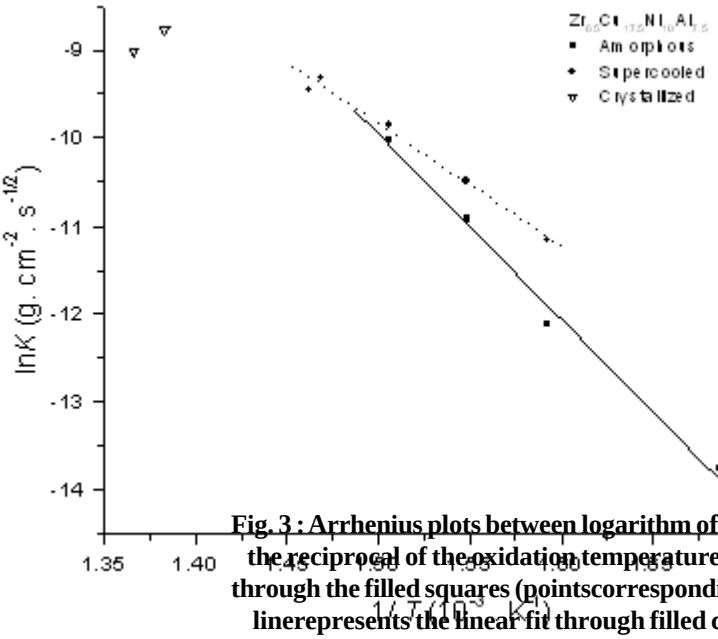

Fig. 3 : Arrhenius plots between logarithm of the parabolic rate constant K [ln$K$ (g.cm-2.sec-1/2)] and the reciprocal of the oxidation temperature T [1/T (10^{-3} K^{-1})].The solid line represents the linear fit through the filled squares (pointscorresponding to the amorphous or the glassy state) while the dotted linerepresents the linear fit through filled circles (points corresponding to the supercooled liquid state).

of Ni in the amorphous state of this alloy ($Zr_{65}Cu_{17.5}Ni_{10}Al_{7.5}$) as reported by Knorr *et al.*, (1999a). It is thus suggessted that the oxidation kinetics for the amorphous state is controlled by the diffusion of Ni and the other alloy constituent Cu whose size does not differ much from that of Cu in the alloy matrix. Our results are supported by similar observations made by Sun *et al.* (1999) for oxidation of amorphous $Zr_{60}Al_{15}Ni_{25}$ in dry oxygen in the temperature range 583 K-683 K.

In contrast, the value of the activation energy in the supercooled liquid state is 1.20 eV which is much less than that of the activation energy in the amorphous state (1.80 eV) indicating that at higher temperatures and for long annealing times when the glass has transformed into supercooled liquid state, the controlling mechanism of oxidation also changes. The value of the activation energy in the supercooled liquid state (1.20 eV) is much different from the value of activation energy for diffusion of Ni in the supercooled liquid state of this alloy (2.9 eV) as reported by Knorr *et al.* (1999a), thus suggesting that back-diffusion of Ni no longer remains the dominant process during oxidation of the alloy in the supercooled liquid state. However, the value of the activation energy (1.20 eV) obtained for oxidation of the supercooled liquid state of the alloy $Zr_{65}Cu_{17.5}Ni_{10}Al_{7.5}$ is close to the activation energy for oxygen diffusion in pure zirconia ZrO_2 (~ 1.0 eV) (Park and Olander, 1991). The small difference in the activation energy values in the two cases may be understood in view of the fact that the alloy investigated here is a multicomponent Zr-based alloy and the oxide film formed has been shown to contain oxide of Al along with the major oxide ZrO_2 (Sharma *et al.*, 2001; Dhawan *et al.*, 2003). Thus it seems more likely that the diffusion of oxygen through the oxide film into the alloy becomes the dominant process for the oxidation of the alloy $Zr_{65}Cu_{17.5}Ni_{10}A_{l7.5}$ in the supercooled liquid state in the temperature range 628-684 K..

Therefore, the values of the activation energy obtained for oxidation of the amorphous (1.8 eV) and the supercooled liquid (1.2 eV) states suggest that the rate controlling process during early oxidation of the amorphous $Zr_{65}Cu_{17.5}Ni_{10}Al_{7.5}$ is the back diffusion of Ni, and possibly Cu also, so long as the alloy remains in the amorphous or the glassy state while at higher temperatures and for longer annealing times when the amorphous or glassy state has transformed into supercooled liquid state, the oxidation is dominated by diffusion of oxygen into the alloy. It is noteworthy here that the suggested mechanisms of oxidation are based on our interpretation of the observed linear regions in mass gain versus square root of oxidation time plots as representing the amorphous and the supercooled liquid states of the alloy $Zr_{65}Cu_{17.5}Ni_{10}Al_{7.5}$ according to the known T-T-T diagram for this alloy and the interpretation of the activation energy values obtained for oxidation of the alloy in the two states.

The above suggested mechanisms were verified by XPS measurements on oxidized specimens. The oxide films formed on the alloy surface as a result of high temperature (in the temperature range 573 K-663 K) oxidation in air were characterized by XPS (Dhawan *et al.*, 2007). The analysis of XPS peaks for constituent elements of the alloy

showed that the ZrO_2 was the major oxide along with a small amount of Al_2O_3 during oxidation in the amorphous state. In this case no Ni or Cu was seen in the oxide film and their presence was noticed only beyond the oxide-alloy interface (Dhawan *et al.*, 2007). On the other hand in the case of oxidation in the supercooled liquid state CuO was present along with ZrO_2 and Ni remained near the oxide-alloy interface due to its slower diffusion rate than that of Cu (Dhawan *et al.*, 2007) and hence its oxidation was suppressed. An understanding about the formation of various oxides on the alloy surface during oxidation in air at various temperatures (in the temperature range 573 K-663 K) can be obtained from the available values for heat of oxide formation. The heats of formation for ZrO_2, Al_2O_3, NiO and CuO are -1101.1, -1117.6, -497.7 and -314.8 KJ/mol O_2, respectively (Lide Ed., 1995-1996). This suggests that oxides of Zr and Al in the alloy $Zr_{65}Cu_{17.5}Ni_{10}Al_{7.5}$ are likely to be formed first because of their strong affinity for oxygen, followed by Ni and Cu. However, the back-diffusion or segregation of alloy constituents during oxidation controls the oxidation kinetics and thus the formation of oxidation products in the oxide film.

In order to clearly highlight these observations depth profiles for the concentration ratio of these elements with respect to Zr in the alloy were obtained and are shown in Figs. 4 and 5. An interesting feature of Fig. 4 pertains to the absence of both Cu and Ni in the oxide film formed at 573 K and 603 K which correspond to the oxidation of the alloy sample in the amorphous state. In contrast, appreciable amount of Cu is seen in the oxide film formed at 633 K and 663 K which correspond to the formation of oxide film in the supercooled liquid state of the alloy. It is interesting to mention here that depth profiles for Al shown

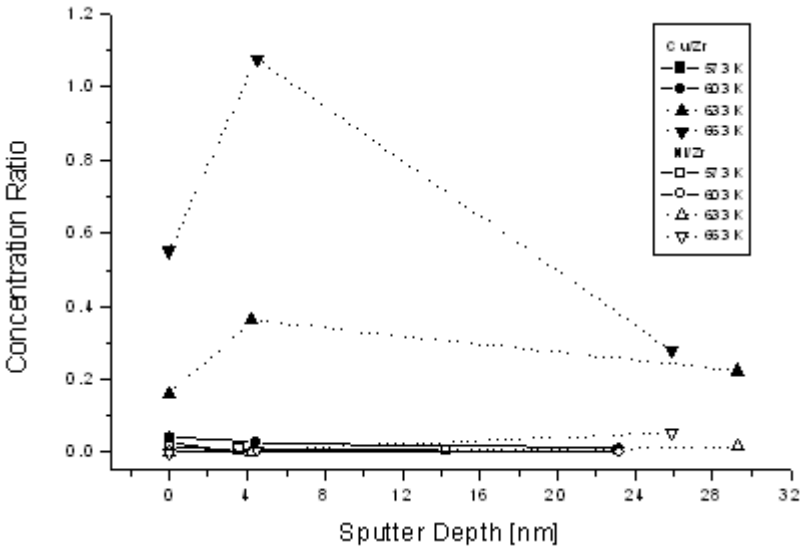

Fig. 4 : Plots of atomic concentration ratio [Cu/Zr] and [Ni/Zr] versus sputter depth for the alloy $Zr_{65}Cu_{17.5}Ni_{10}Al_{7.5}$ oxidised at different oxidation temperatures.

Fig. 5 : Plots of atomic concentration ratio [Al/Zr] versus sputter depth for the alloy $Zr_{65}Cu_{17.5}Ni_{10}Al_{7.5}$ oxidised at different oxidation temperatures.

in Fig. 5 are in sharp contrast with those for Cu (Fig. 4). Al is present on the surface after oxidation at all temperatures, but hardly any Al is seen deeper in the oxide film formed at higher temperatures, i.e. at 633 K and 663 K (Fig. 5). It is very likely that due to strong segregation of Cu at these temperatures (Fig. 4) the relative concentarion of Al in the oxide film containing Zr and Cu becomes too low to yield a significant XPS peak of Al. The role of Cu and Ni is explained by the controlling oxidation mechanisms and is discussed in the following paragraphs.

It is, thus, suggested from the above discussion that the depletion of Ni and Cu in the oxide film, as seen in Fig. 4, possibly arises due to their back diffusion into the alloy during oxidation of the alloy and the absence of these elements (Ni and Cu) in depth profiles after oxidation of the alloy specimen in the amorphous state can be understood. As the alloy reaches the supercooled liquid state during oxidation (at temperatures 633 K and 663 K) strong segregation of Cu is noticed in the oxide film (Fig. 4) which point to a change in the mechanism of oxidation of the alloy in its supercooled liquid state, i.e. the oxidation mechanism is dominated by the inward diffusion of oxygen than the back diffusion of Ni and Cu into the alloy (Sun X. *et al.*, 1996; Dhawan A. *et al.*, 2001 and 2003). During oxidation of the alloy the rate controlling process is the back diffusion of Cu and Ni so long as the alloy remains in its amorphous state (which can be ascertained fom the known T-T-T diagram of the alloy (Knorr K., 1999) and it is most likely that Cu, being a slower diffuser than Ni, is present closer to the oxide-alloy interface than Ni and thus gets easily oxidized at 633 K and 663 K when the alloy attains the supercooled liquid state after initial oxidation. In the supercooled liquid state the oxide film formation is dominated by the inward diffusion of oxygen anions and outward diffusion of cations of zirconium and copper.

The diffusion rates of smaller atom (Cu here) are, in fact, about two orders of magnitude larger at temperatures of interest in the supercooled liquid state (633 K and 663 K) than that in the amorphous state (573K and 603 K) (Faupel F. *et al.*, 2003; Hahn H. *et al.*, 19888; Sharma S. K. *et al.*, 1989). This facilitates the outward diffusion of Cu and its consequent oxidation by inwardly moving oxygen atoms. Moreover, the larger amount of Cu (17.5 at.%) in the alloy than Ni (10 at.%) and the proximity of the former to the oxide-alloy interface after the initial oxidation till the alloy remained in the amorphous state are the favourable factors leading to the oxidation of Cu and the corresponding suppression of the oxidation of Ni in the supercooled liquid state of the alloy specimen. This explains the absence of Ni in depth profiles for oxidation of the alloy in the supercooled liquid state (Fig. 4).

Therefore, the observations reported in this study support the view that different oxidation mechanisms are operative for oxidation of the alloy $Zr_{65}Cu_{17.5}Ni_{10}Al_{7.5}$ at low temperatures (corresponding to the amorphous state of the alloy) and at high temperatures (corresponding to the supercooled liquid state of the alloy).

Zr-based bulk amorphous alloys are known to exhibit nanocrystalline phases after thermal annealing (Koester U. and Triwikantoro, 1999; Spassov T. and Tzolova G., 1996). Few investigations on oxidation of Zr-based nanocrystalline alloys have been reported in the literature (Koester U. *et al.*, 1999; Koester *et al.*, 2001; Spassov T. and Tzolova G., 1996). Koester *et al.* (1999 and 2001) have shown that during oxidation of several Zr-based nanocrystalline alloys the oxidation of amorphous alloy was much faster compared to its nanocrystalline counterpart. In another investigation on amorphous and nanocrystalline $Zr_{67}Co_{33}$ (Spassov T. and Tzolova G., 1996) it has been reported that the oxidation rate for the nanocrystalline phase is lower than that for he amorphous phase of the same alloy. These results are very important and are suggestive of the fact that Zr-based nanocrystalline alloys may have better oxidation resistance than their amorphous counterparts. However, more investigations on comparative behaviour of oxidation of amorphous and nanocrystalline alloys are much desired in order to prove that Zr-based nanocrystalline alloys are more oxidation resistant than their amorphous counterparts. A correlation of the oxidation behaviour with the structure of nanocrystalline phases will be very useful in understanding the differences in oxidation behaviour of these alloys.

Conclusions

The results of oxidation of the bulk amorphous alloy $Zr_{65}Cu_{17.5}Ni_{10}Al_{7.5}$ carried out in air in the temperature range 573 K-663 K revealed the following:

1. The oxide film contained ZrO_2 as the major constituent along with some Al_2O_3 and CuO. No Ni and Cu were detected in the oxide film formed at 573 K and 603 K (corresponding to the amorphous state of the specimen) while appreciable amount of Cu (as CuO) was found in the oxide film formed at 633 K and 663 K (corresponding to the supercooled liquid state). In the later case no Ni was detected due to strong segregation of Cu (Cu being present in much higher concentration in the alloy than Ni) and the proximity of Cu to the oxide-alloy interface.

2. The above results are consistent with the previously proposed mechanism for the

air oxidation of this alloy suggesting that the rate controlling process during the oxidation of the alloy at low temperatures (in the amorphous state) is the back diffusion of Ni and Cu while the oxidation at higher temperatures (in the supercooled liquid state) is dominated by the inward diffusion of oxygen and the outward diffusion of zirconium and copper.

3. Different oxidation behaviours have been observed amorphous and nanocrystalline alloys of the same composition. More investigations on better oxidation resistance of nanocrystalline alloys than their amorphous counterparts are required to establish the superiority of the former so far as their oxidation is concerned.

Acknowledgements

Thanks are due to my co-workers Dr. F. Faupel, Dr. V. Zaporotchenko, and Dr A. Dhawan. The help provided by Ms Jugrita Zekonyte and Mr. Stefan Rehders during XPS measurement is gratefully acknowledged. A part of the work was carried out during the research project from the Board of Nuclear Sciences (BRNS Grants No. 99/37/25/BRNS) for which the financial funding is gratefully acknowledged.

References

Asami K., Kimura H. M., Hashimoto K. and Masumoto T. (1995): *Mat. Trans. JIM*, **36**, 988.

Dhawan A., Raetzke K., Faupel F. and Sharma S. K. (2003): *phys. stat. sol. (a)*, **199**, No. 3, 431-438.

Dhawan A., Raetzke K., Faupel F. and Sharma S. K. (2001), *Bull. of Mater. Sci*., **24**, 281.

Dhawan A., Zaporojtchenko V., Faupel F. and Sharma S. K. (2007): *J. Mater. Science* (in press).

Faupel F., Frank W., Macht M.-P., Mehrer H., Naundorf V., Raetzke K., Schober H. R., Sharma S. K. and Teichler H. (2003): *Reviews of Modern Physics*, **75**, 237.

Hahn H., Averback R. S. and Shyu H. -M. (1988): *J. Less-Common Met.*, **140**, 345.

Hashimoto K. (1983):, in "*Amorphous Metallic Alloys*", (Ed.) F. E. Luborsky (Butterworths, London) p.471.

Johnson W. L. (1996): Current Opinion in *Solid State Mater Science*, **1**, 383.

Kiene M., Strunskus T., Hasse G. and Faupel F. (1999): in "*Bulk Metallic Glasses*", W. L. Johnson, C. T. Liu and A. Inoue (Eds.), MRS Symposia Proceedings No. 554 (Materials Research Society, Pittsburgh) p. 167.

Knorr K. (1999): in "*Selbstdiffusion in Metallischen Massivglaesern*",Ph.D thesis, University of Muenster, Muenster, Germany.

Knorr K., Macht M. -P.and Mehrer H. {1999): in "*Bulk Metallic Glasses*", W. L. Johnson, C. T. Liu and A. Inoue (Eds.), MRS Symposia Proceedings No. 554 (Materials Research Society, Pittsburgh) p. 269.

Koester U. and Triwikantoro (1999): *Mater. Sci. Forum*, **360-362**, 29.

Koester U., Zander D., Leptien H., Eliaz N. and Eliezer D. (1999): in "*Bulk Metallic Glasses*", W. L. Johnson, C. T. Liu and A. Inoue (Eds.), MRS Symposia Proceedings No. 554 (Materials Research Society, Pittsburgh) p. 287.

Koester U., Zander D., Triwikantoro, Ruediger A. and Jastrow L. (2001): *Scripta Materialia*, **44**, 1649.

Lide D. R. (Ed.): in "*CRC Handbook of Chemistry and Physics*", 76th Edition (1995-1996): (CRC Press, Boca Raton) pp. 34-47.

Park K. and Olander D. R. (1991): *J. Electrochem. Soc*., **138**, 1154.

Sharma S. K., Banerjee S., Kuldeep and Jain A. K. (1989): *J. Mater. Res*., **4**, 603.

Sharma S. K., Strunskus T., Ladebusch H.and Faupel F. (2001): *Mater. Sci. Eng. A*, **304-306**, 747.

Spassov T. and Tzolova G. (1996): *Cryst. Res. and Tech*., **37**, 881.

Sun X., Schneider S., Geyer U., Johnson W. L.and Nicolet M-A. (1999): *J. Mater. Res*., **11**, 2738.

Tam C. Y. and Shek C. H. (2005): *J. Mater. Res*., **20**, 1396.

Triwikantoro, Toma D., Meuris M., Koster U. (1999): *J. Non-cryst. Solids*, **250-252**, 719.

Zhang T., Inoue A. and Masumoto T. (1991): *Mater. Trans. JIM*, **32**, 1005.